Increasing land take in Europe's land-water interface

Xiang Liu [1,2*], Tobias Kuemmerle [1,3], Matthias Baumann [1], Shawn Schneidereit [1] & Sonja C. Jähnig [1,2]

[1] Geography Department, Humboldt-Universität zu Berlin, Unter den Linden 6, Berlin, 10099 Germany

[2] Leibniz Institute of Freshwater Ecology and Inland Fisheries, Müggelseedamm 310, Berlin, 12587 Germany

[3] Integrative Research Institute on Transformations of Human-Environment Systems (IRI THESys), Humboldt-University, Berlin, Germany

* Corresponding author: xiang.liu@geo.hu-berlin.de

Summary

Ecosystems at the interface between terrestrial and aquatic areas are of outstanding ecological and socio-economic importance, yet are under intense pressure due to the concentration of human settlement and agriculture. Despite this, the broader geography of the land-water interface and how it is changing remains poorly understood. Here, we develop an operationalizable definition of the land-water interface and use a fuzzy logic geospatial model to map the land-water interface at high resolution across the European continent. Our results show that the land-water interface covers ~0.87 million km² (~8% of Europe) but is strongly affected by human use: in 2020, about 15% of all built-up areas and more than 8% of all croplands lay within the land-water interface. Analyzing land-cover trends inside the land-water interface since 1992 showed increasing land take: built-up area more than doubled (from 13,752 km² to 29,302 km²), driven primarily by cropland-to-urban conversion. The expansion and densification of built-up areas occurred particularly in lowland river corridors, deltas, and coastal plains. Cropland decline was particularly widespread across Central and Eastern Europe, while cropland expansion occurred in land-water interface regions in northern Europe. Across interface types, the lake land-water interface exhibited the strongest relative increase in built-up areas (>150%) and the sharpest proportional cropland loss compared to riverine and coastal land-water interfaces. Countries inside the European Union had earlier and more intense urbanization trends than non-EU regions, with a slowdown after 2010. More broadly, our results reveal a continental-scale pattern of increasing, and largely irreversible, land take in the land-water interface, likely straining the ecological integrity, buffering capacity, and connectivity of land-water ecosystems. Our land-water interface concept and harmonized maps enable consistent mapping and regional cross-comparisons, support identification of priority areas for conservation and restoration, and provide a baseline to track progress towards flood-risk reduction and restoration targets.

Keywords

Land-water interface; Rivers; Urbanization; Agriculture; Land-use change; Wetlands; Remote sensing; European Union

Introduction

Where land and water meet, ecotones emerge that contain properties of both terrestrial and aquatic ecosystems (Downing et al., 1993). Examples of such interfaces include riverbanks, lakeshores, wetlands, and coastal zones. These ecosystems are widely recognized for being among Earth's most fertile and biologically productive landscapes, characterized by intensive biogeochemical cycling and high biodiversity (Karr & Schlosser, 1978; Ward et al., 2002). The land-water interface is also extraordinarily important for providing ecosystem services, including the mitigation of flood risk (Grabowski et al., 2022), the provision of freshwater and food (e.g., fish, crops) (Grabowski et al., 2022; Ward et al., 2002), or for recreation and tourism (Hall, 2001).

As a result, the land-water interface has been preferred by people since the onset of human civilization, subjecting it to growing anthropogenic pressure. The land-water interface now hosts a disproportionately large share of human populations, settlements, and agriculture (Downing et al., 1993; Grabowski et al., 2022). For instance, globally, approximately 10% of the population resides in low-elevation coastal zones (MacManus et al., 2021), with urban areas expanding faster near estuaries and coastlines than elsewhere (Neumann et al., 2015). Similarly, settlements, urban sprawl, and recreational homes expand along inland waters such as rivers and lakes (Rajib et al., 2023). Likewise, approximately 3.4 million km² of inland wetlands have been lost over the past three centuries, predominantly converted to cropland (Fluet-Chouinard et al., 2023), severely undermining the ecosystem services they provide. Together, this renders land-water interface areas particularly vulnerable to human pressure (Capon et al., 2013; Fernandes et al., 2016). Clearly, sustainability planning and policies are increasingly critical for land-water interfaces, as population growth, consumption patterns, and urbanization intensify, and climate change progresses (MacManus et al., 2021; Rajib et al., 2023).

Despite this, these interfaces have historically been neglected, as research has often compartmentalized terrestrial and aquatic ecosystems, overlooking their transitional boundaries (Campbell et al., 2022; Fluet-Chouinard et al., 2023; Pekel et al., 2016). Processes such as sediment transport, nutrient exchange, or species' movements and migration transcend the land-water divide, yet these interactions are rarely considered explicitly (Altanov et al., 2025; Grabowski et al., 2022). One reason is that the terrestrial and aquatic parts of the land-water interface tend to be studied in isolation or as part of highly abstracted, broader geographic units (e.g., as part of hydrological systems or watersheds; Naiman et al. 2010, Acreman and Holden 2013). Likewise, policies and ecosystem management also often focus on only one of the subsections. For instance, when managed solely from a hydrological engineering perspective, aquatic and terrestrial subsystems tend to become disconnected, diminishing their role in nutrient retention and flood regulation (Chipps et al., 2006; Verhoeven et al., 2006). Finally, land-water interfaces are rarely considered

explicitly in broad-scale mapping exercises, with their respective subsystems assigned to broader terrestrial or aquatic land-cover classes (e.g., riparian forests to broadleaved forests; Johansen et al., 2010), in part because of spectral similarities that make it challenging to disentangle transitional zones from surrounding land covers (Fernandes et al., 2013; Weissteiner et al., 2016). Our understanding of the geography of the land-water interface, and how it has been changing, is therefore overall weak.

A critical barrier in this context lies in the absence of a standardized and operationalizable definition that would allow a consistent mapping of these interfaces. Existing frameworks, such as the EU Water Framework Directive and the Ramsar Convention (1971), prioritize water bodies or wetland habitats (i.e., neglect areas on land connected to these ecosystems), and fail to delineate land-water interfaces as interconnected systems (González del Tánago et al., 2021; Schweizer et al., 2022). Similarly, global surface water datasets omit transitional buffers and the terrestrial subsystems of the land-water interface (Pekel et al., 2016). Definitions for some land-water interfaces, such as riparian zones, exist but vary hugely, from as narrow as 10 m to as broad as 1 km (Fischer & Fischenich, 2000). Moreover, such definitions have focused on certain freshwater ecosystems, often rivers, while neglecting others, such as lake margins, wetland edges, and coastal transition zones (Grabowski et al., 2022). There are many calls for a more holistic governance of human pressures in interface areas (Grabowski et al., 2022; Pace et al., 2022), yet without a harmonized definition, quantifying the extent of the land-water interface, monitoring trends within it, and designing interventions targeted at maintaining its ecological integrity and ecosystem services remains challenging.

Pressure on the land-water interface is particularly intense in regions with long land-use histories, such as Europe (Kastner et al., 2022; Kuemmerle et al., 2016). Here, floodplains, coastal zones, and lakeshores have been subject to settlement and agricultural exploitation for millennia, resulting in the widespread transformation of natural ecosystems (Tockner & Stanford, 2002). For instance, up to 90% of historical floodplains have been transformed through agricultural expansion and urbanization (EEA, 2020b). In recent decades, increasingly divergent land-use trajectories have emerged across the continent, with an intensification and expansion of agriculture on the one hand, and the de-intensification of abandonment of agricultural areas on the other (Kastner et al., 2022; Kuemmerle et al., 2011). These dynamics exhibit high spatial variability. Agricultural abandonment is notably more prevalent in non-EU countries, particularly across Eastern Europe, following the collapse of the former Soviet Union and with it socialist farming systems (Estel et al., 2015; Schierhorn et al., 2013). Conversely, land-use patterns within the EU have been predominantly shaped by successive Common Agricultural Policy (CAP) reforms and bioenergy directives, which have significantly influenced land management (Levers et al., 2018). This concentration of production in high-yield, profitable landscapes, particularly fertile floodplains, has likely placed

disproportionate pressure on the land-water interface (Kuemmerle et al., 2016), yet land-use trends within these ecotones remain poorly understood. This knowledge gap is critical, as permanent land conversion within these interfaces has compromised natural flood resilience at a time when climate change is increasing European flood risk (Jongman et al., 2014). Ecological restoration of the land-water interfaces in Europe is thus important, but hinges on a better understanding of how agricultural change and urbanization have impacted it.

In this study, we address these gaps by leveraging high-resolution geospatial data on land use and land cover. To this end, we have developed an operationalizable definition of the land-water interface and have mapped it at 30-meter resolution across the European continent. Based on this, we quantified the extent and spatial patterns of urbanization and cropland change inside the land-water interface for the period 1992 to 2020. Specifically, we ask:

1. What is the spatial extent and geographic distribution of the land-water interface across Europe?
2. How have built-up and cropland changed inside the land-water interface since 1992?
3. How do land-use changes inside land-water interface areas differ inside and outside of the European Union, as well as between river, lake, and coastal land-water interfaces?

Results

Europe's land-water interface

Across Europe, the total extent of the land-water interface was about 870,050 km² (~8% of the European land area). High densities of land-water interface occurred, expectedly, along coastal zones and in major river corridors (e.g., the Danube, and the Rhine-Meuse-Scheldt delta/lowlands, as well as the Vistula and Elbe valleys). Interface areas were also widespread in lake-rich regions (e.g., Fennoscandia and parts of the Alpine forelands) and locally, in dissected terrains where dense river networks are found (Fig. 1A–G). Among interface types, riverine land-water interface dominated (~4.0% of area), followed by lake land-water interface (~2.4%) and coastal land-water interface (~1.6%; Fig. 1H). Across biomes, the river land-water interface dominates (about 1.7–7.6%), while coast land-water interface was consistently small (roughly 0.2–4.3%; Fig. 1I). The highest overall shares of land-water interface occurred in Tundra (~14.4%), followed by Deserts & Xeric Shrublands (~13.8%), Boreal Forests/Taiga (~9.2%), Temperate Grasslands/ Shrublands (~8%), Temperate Broadleaf & Mixed Forests (~6.8%), Mediterranean Forests, Woodlands & Scrub (~4.1%), and the lowest share in Temperate Conifer Forests (~2.8%). Lake land-water interface was

especially important in the Tundra (~6.5%) and Boreal/Taiga (~4.7%) biomes, but generally lower (~0.8–1.6%) elsewhere.

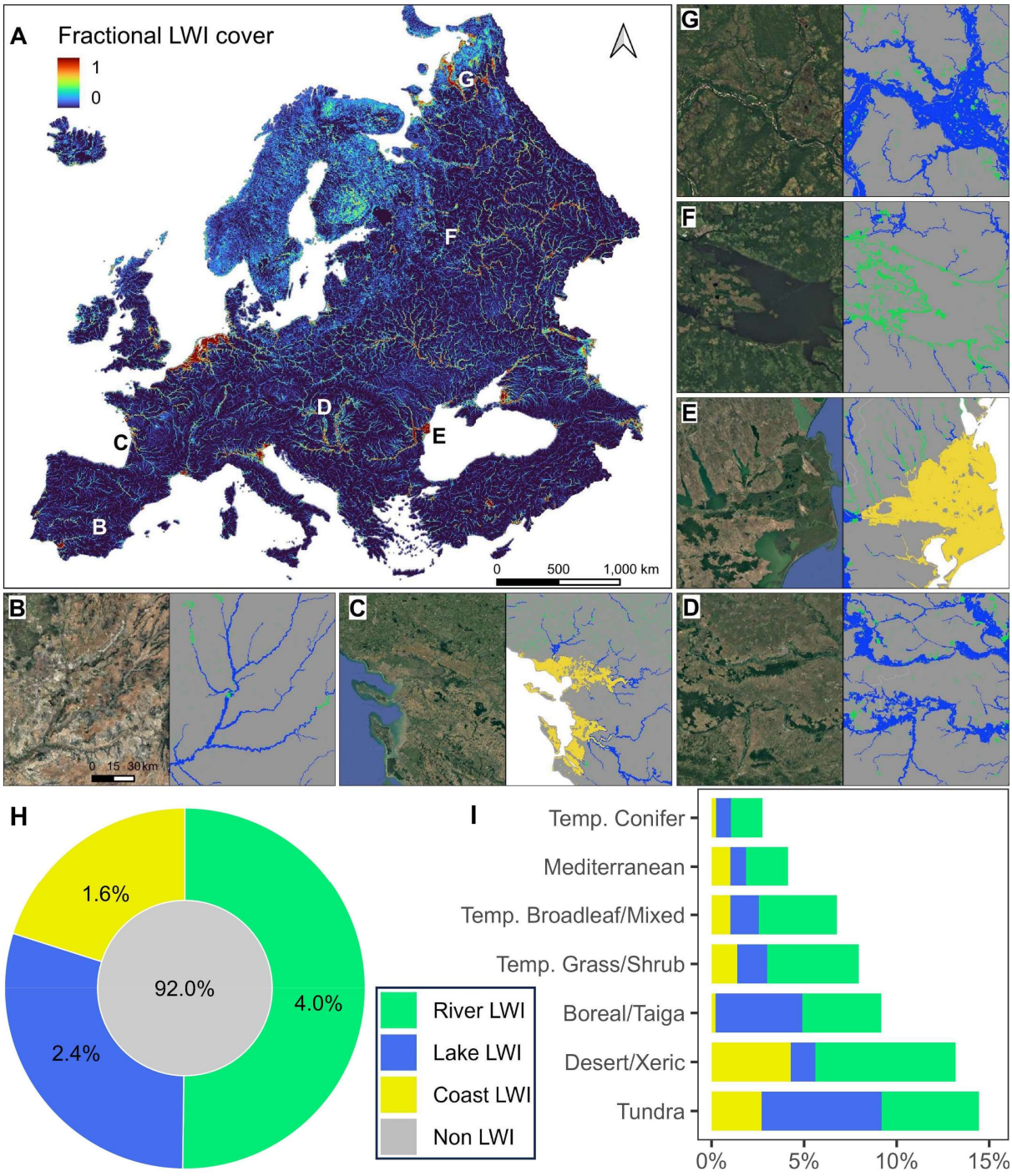

Figure 1. Distribution of the land-water interface (LWI) in Europe. (A) Share of LWI in 3-km grid cells, aggregated from the native 30-m resolution LWI map for visualization purposes. (B–G) Examples of the native, high-resolution LWI maps. (H) Proportion of the European land area classified as coastal, river, and lake LWI. (I) Share of coastal,

river, and lake land-water interfaces of biomes (Boreal Forests/Taiga; Deserts & Xeric Shrublands; Mediterranean Forests, Woodlands & Scrub; Temperate Broadleaf & Mixed Forests; Temperate Conifer Forests; Temperate Grasslands & Shrublands; and Tundra).

Land take in the land-water interface

Europe's land-water interface was dominated by cropland and forest, according to our analyses (Fig. 2A). Importantly, the proportion of cropland within the land-water interface declined slightly from 32.61% in 1992 to 31.64% in 2020 (Fig. 2A), representing about 10,440 km² (Fig. 2B). At the same time, built-up area in the land-water interface more than doubled from 13,752 km² in 1992 to 29,302 km² in 2020. Notably, the land-water interface accounted for approximately 15% of Europe's total urban area (Fig. S1). Cropland net loss and built-up area net gain were the most pronounced land-cover changes in the land-water interface (Fig. 2C).

Transition analysis further revealed that built-up expansion within the land-water interface was indeed mainly happening on former cropland (Fig. 2D). Built-up gains peaked during 2000–2010, when more than 6,000 km² of cropland was converted to urban land, with gain intensities exceeding 0.17% yr^{-1}. Although urban expansion slowed during 2010–2020, it continued to occur primarily at the expense of cropland (Fig. 2D−E). In contrast, cropland gains within the land-water interface weakened over time and were mainly derived from conversions of forest and grassland (Fig. S2). Together, these results highlight that cropland-to-urban conversion was the principal process of land transformation in Europe's land-water interfaces in the last decades.

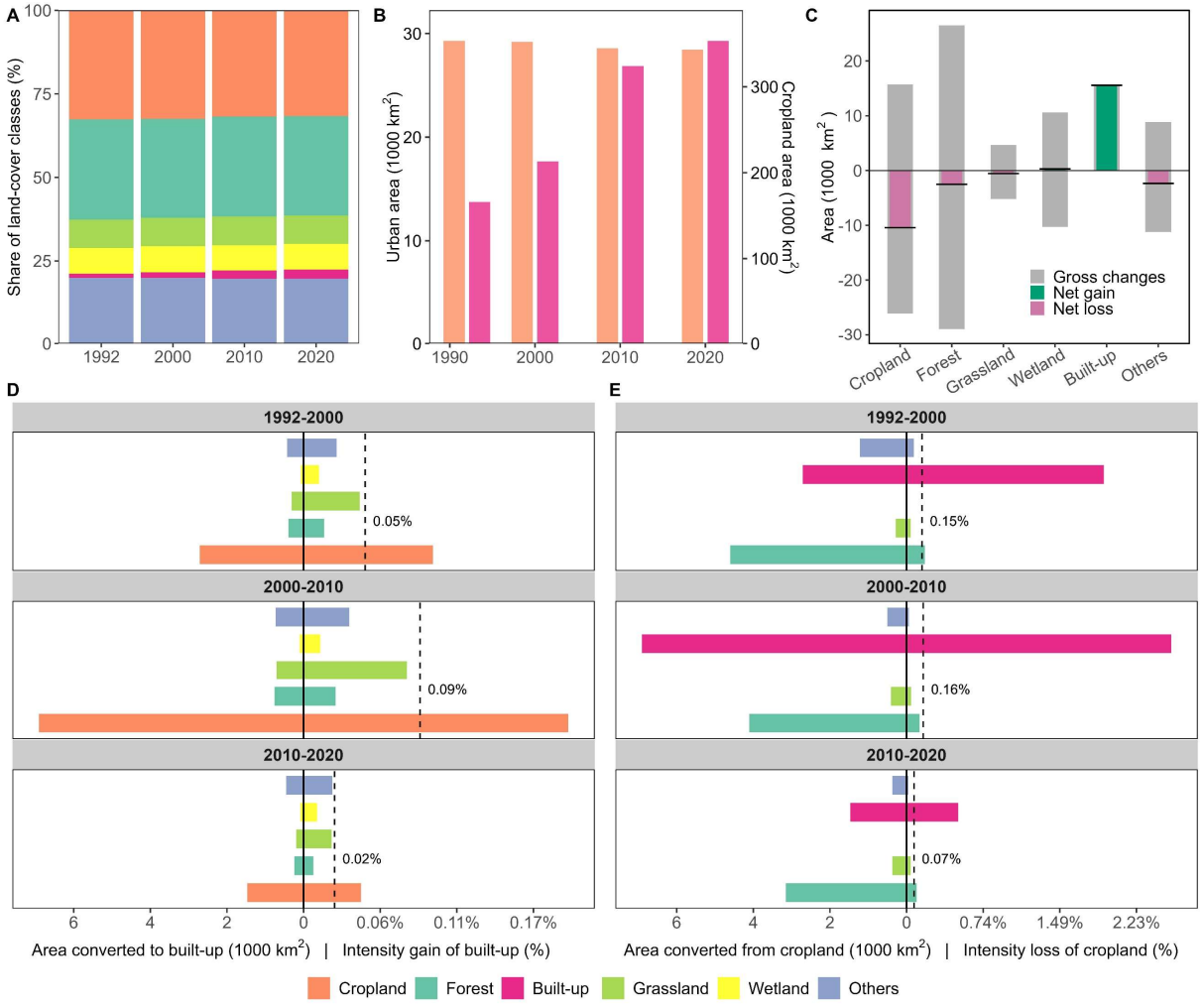

Figure 2. Land-cover composition and major land-cover transitions in Europe's land-water interface (LWI) between 1992 and 2020. (A) Share of land-cover classes in the LWI. (B) Changes in urban areas and cropland in the LWI. (C) Gross and net changes by land-cover types. (D) Gains of built-up areas and their intensities. (E) Loss of cropland and its intensity. The uniform rate line (vertical dashed line; value shown in each time interval) indicates the constant (period-average) intensity expected under a uniform-rate assumption, and serves as a benchmark for comparing class-specific intensities.

Analyzing the spatial patterns of land transformations across Europe's land-water interfaces from 1992 to 2020 showed contrasting patterns (Fig. 3A–B). Built-up density rose strongly along lowland river corridors, deltas, and coastal zones in Western and Central Europe, especially around major urban agglomerations in the Rhine, Po, and Danube basins, with hotspots in floodplains and coastal lowlands. Built-up areas within all land-water interface types expanded steadily, with lake land-water interfaces exhibiting the strongest relative increases, exceeding 150% growth (Fig. 3C). Compared to non-land-water

interface areas, all land-water interface types experienced stronger relative expansion. Cropland density within land-water interface zones declined broadly across much of Central and Eastern Europe, while gains were spatially patchy and most evident in parts of northern Europe (notably Fennoscandia) and in scattered areas toward eastern Europe/Russia (Fig. 3B). Many mountainous regions exhibited comparatively weak or localized changes. Cropland area declined across all land-water interface types, most sharply within lake land-water interfaces (Fig. 3D).

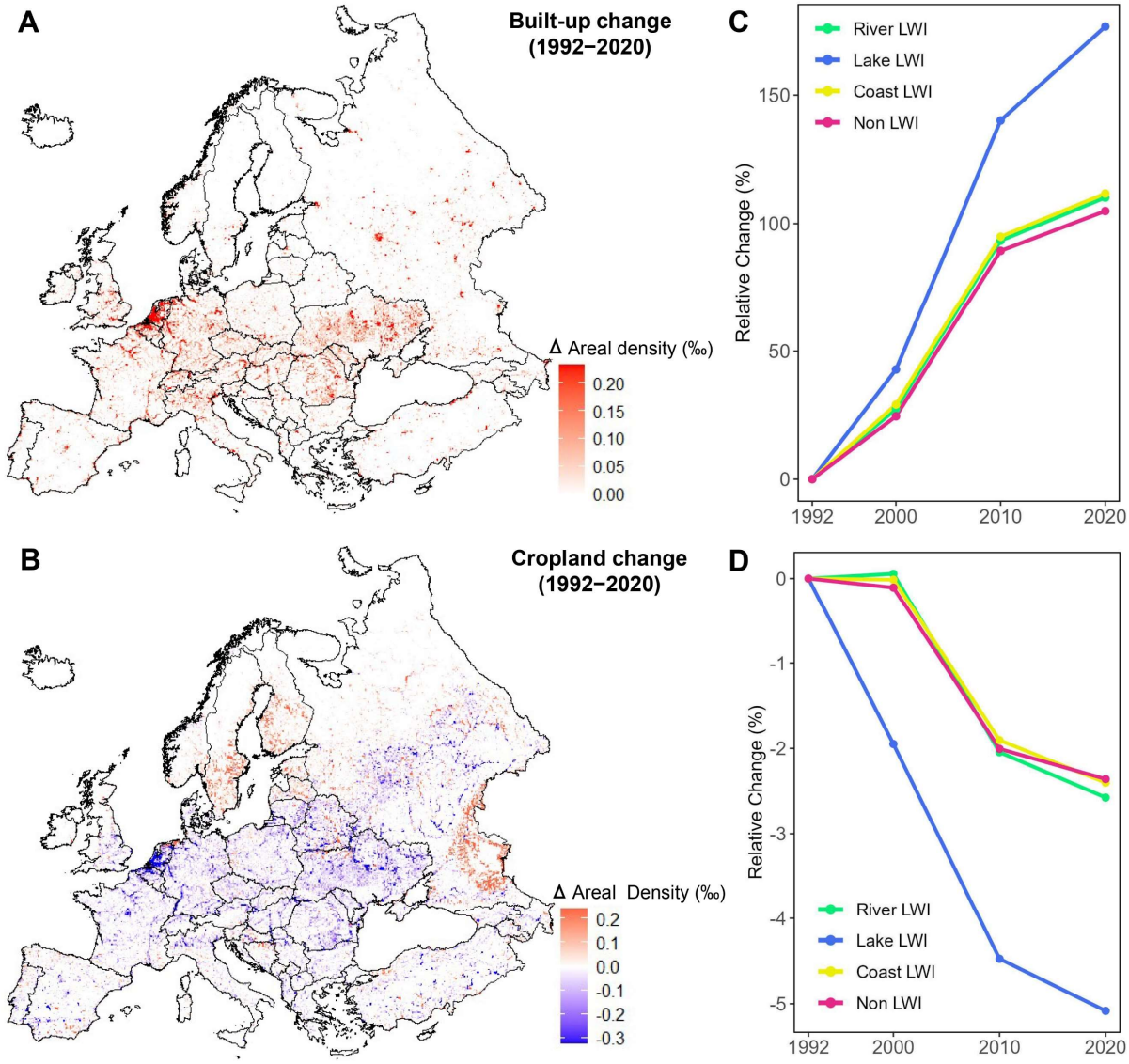

Figure 3. Built-up and cropland change inside Europe's land-water interfaces (LWIs) between 1992 and 2020. (A) Changes in built-up areal density. (B) Changes in cropland areal density. (C) Relative change in built-up areas (%) since 1992. (D) Relative change in cropland area (%) since 1992.

Land transformations within the land-water interface inside and outside the EU+

Within the EU+, the land-water interface had consistently higher fractions of grassland, cropland, and urban land than in the non-EU+ region (Fig. 4A–B). Built-up area expanded in both regions, with a larger absolute increase in EU+ than in non-EU+ (≈ 9,884 km² vs 5,673 km², Fig. 4C). In contrast, cropland area remained consistently higher in non-EU+ than in EU+ throughout the period, while both regions experienced only modest cropland declines (≈ 188, 320–184,100 vs 165,676–159,443km², Fig. 4D). In both regions, built-up expanded mainly over cropland in the land-water interface (Fig. 4E–F), but urbanization intensity was higher inside the EU+ than outside. In terms of cropland change, cropland primarily transitioned to either forest or built-up areas in both regions, with loss intensity peaking during 2000–2010 (Fig. 4G–H). Together, this reveals a synchronized yet more pronounced pulse of urbanization and cropland decline in EU+ landscapes, whereas non-EU+ interfaces display a similar but more subdued pattern of change.

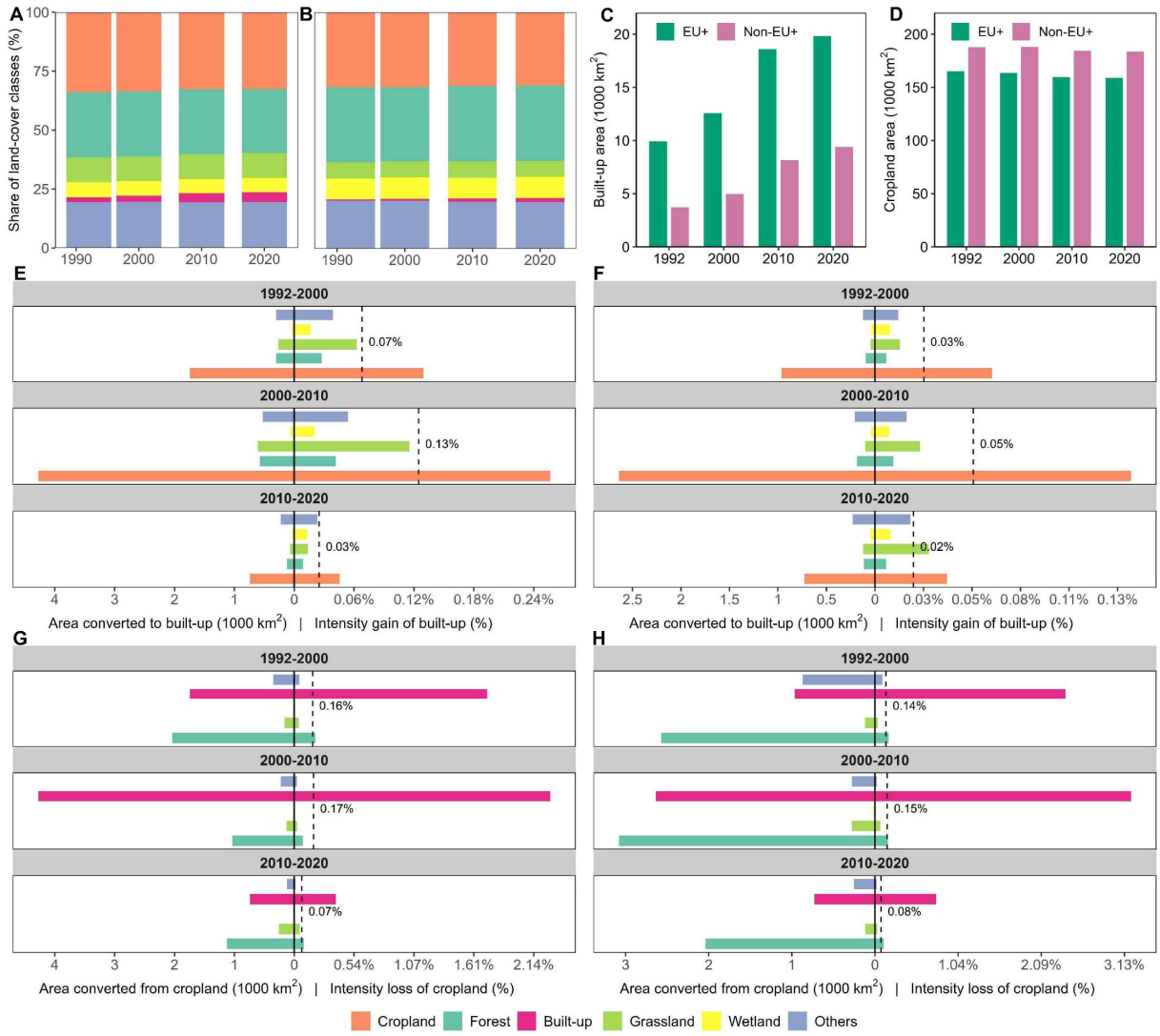

Figure 4. Land-cover transformations in the land-water interface (LWI) of Europe union plus (EU+) and non-EU+ regions from 1992 to 2020. (A–B) Share of major land cover classes. (C–D) Area changes of cropland and built-up land. (E–F) Transition gains to built-up land and their corresponding intensities. (G–H) Transition losses from cropland and their intensities. The uniform rate line (vertical dashed line; value shown in each time interval) indicates the constant (period-average) intensity expected under a uniform-rate assumption, and serves as a benchmark for comparing class-specific intensities.

Discussion

The interfaces between terrestrial and aquatic ecosystems are important transitional zones that function as critical regulatory hubs and provide important habitat for a wide range of species (Grabowski et al., 2022; Weissteiner et al., 2016). Beyond their ecological importance, land-water interfaces deliver substantial

societal benefits. As highly productive ecosystems, they supply numerous ecosystem services, store and sequester substantial amounts of carbon, and, perhaps most importantly, play a crucial role in mitigating flood risk (Ervin & Wetzel, 2003; Tellman et al., 2021; Tockner & Stanford, 2002). However, land-water interfaces are under high and rising human pressure. A long history of settlement, agriculture, and infrastructure development in them have led to their transformation and degradation in many regions (Rajib et al., 2023), including in Europe, where it is estimated that 70–90% of floodplains (EEA, 2020b), and 60% of peatlands have been degraded (Wetlands International Europe, 2025), and >80% of river, lake, and riparian habitats are in unfavorable condition (Bastino et al., 2021). Despite this, land-water interfaces have been a blind spot in both science and governance, with the focus often on either the terrestrial or aquatic parts of interfaces. Here, we address two major gaps in this context. First, we developed a harmonized, generic, and operational definition of land-water interfaces and, second, provided a high-resolution spatial baseline map of these interfaces at the continental scale. We demonstrate the usefulness of this map by assessing how urbanization and agricultural land-use change have transformed the land-water interface in Europe in the period 1992 to 2020. This yielded three main insights.

First, we show that the European land-water interface constitutes an extensive socio-ecological corridor covering almost 0.87 million km². While representing only 8% of the continent's area, these zones host an intensive concentration of human activities, encompassing roughly 15% of all built-up land and over 8% of European cropland (Fig. S1). This spatial concentration is a direct legacy of a long settlement history rooted in the exceptional productivity and connectivity of these zones. For millennia, European communities were drawn to these "riverscapes" to exploit the "meadow economy," in which seasonal floods provided nutrient-rich silt for high-quality grazing and hay, alongside protein from rich fisheries and vital trade access (Firth et al., 2026; Hoffmann, 2005; Tesselaar et al., 2023). As these productive areas were the first to be settled, they established a path dependency that continues to determine much of today's settlement patterns (Tesselaar et al., 2023). It is estimated that approximately one in eight Europeans currently lives on flood-prone land, despite floodplains comprising only approximately 7% of European territory (Christiansen et al., 2019). This historical attraction was followed by a large-scale engineering push during the 18th–20th centuries, designed to make these lands more accessible by controlling flow regimes and draining vast floodplain areas (Gatejel, 2025; Wolf et al., 2021). During these periods, wetlands were increasingly viewed as "mistakes of nature" or "wastelands" that impeded progress and bred disease (Bruisch, 2020). Technological advancements, such as the introduction of steam-powered dredges in the mid-19th century, allowed for the systematic canalization of rivers and massive reclamation schemes like those in the Rhine, Oderbruch and the Po Valley (Brandolini & Cremaschi, 2018; Quast, 2005). This era of "productivism," often fueled by 20th century government subsidies, resulted in the loss of approximately

80% of European wetlands, replacing dynamic ecotones with stabilized landscapes that facilitate shipping and rail networks but lack natural structural resilience (Verhoeven, 2014).

More recently, the primary driver for water-proximate living has undergone a significant "amenity transition," where proximity to lakes, coasts, and rivers is valued for its recreational, aesthetic, and cultural significance rather than its relative productivity (Gosnell & Abrams, 2011). This shift is characterized by the growing importance of second homes, which now account for more than 25% of the housing stock in Alpine resort communities (Sonderegger & Bätzing, 2013) and over 25% in Mediterranean coastal provinces like Alicante (Valenzuela-Martin et al., 2025). Our analysis uncovers major spatial nuances in these transformations; while coastal and riverine zones have been focal points for millennia and were already heavily built up by the late 20th century (Kasanko et al., 2006; Rosati, 2025), traditionally "remote" lake shorelines and smaller wetlands are now facing a sharp uptick in human pressure. Lake-associated land-water interfaces experienced the most intense relative urban growth since 1992 (Fig. 3B), representing a rapid percentage increase on a previously low-developed base (Fig. S3). This pattern is vividly illustrated in the Polish and Hungarian lake districts, where shorelines once dominated by natural vegetation or cropland have seen a boom in resorts, marinas, and tourism infrastructure (Furgała-Selezniow et al., 2020, 2022). In the catchment of Lake Balaton, mass tourism has driven significant urban expansion over recent decades, demonstrating that even isolated interfaces are now squarely in the path of development (Petrovszki et al., 2024). Any effective conservation or spatial planning strategy will therefore need to account for such spatial nuances, balancing the longstanding urban-industrial pressures on big rivers and coasts with the newly emerging hotspots of change in lake and wetland regions.

Second, we found a major increase in built-up areas, which more than doubled from 1992 to 2020, resulting in land transformations that have affected over 13,752 km^2 within Europe's land-water interface. This rapid expansion has been disproportionately concentrated on high-productivity croplands, which are among the most fertile and biodiverse ecosystems worldwide (Gardi et al., 2015). The systematic sealing of these prime soils is concerning because it creates a "leakage" effect: as these fertile European floodplains are lost to development, agricultural production is often displaced to other European regions, potentially triggering the destruction of primary forests or the cultivation of marginal lands to maintain the global food supply (Bren d'Amour et al., 2017; Yang et al., 2026). This trend reflects a critical mismatch where economic development and urban sprawl occur at the expense of non-renewable agricultural resources and regional food security (van Vliet et al., 2017). Furthermore, converting agricultural and natural landscapes into urban areas replaces permeable soils with impervious surfaces, which significantly lowers the landscape's natural water-storage potential and resilience to both floods and droughts (Andreadis et al., 2022; Halecki & Młyński, 2025).

Beyond the physical disruption of the water cycle, this transformation introduces a complex trade-off in water quality (Giri & Qiu, 2016). While the volume of agricultural nutrients like nitrogen might decrease, it is replaced by urban micropollutants, including pharmaceuticals, industrial chemicals, and microplastics. This largely irreversible land take is therefore likely to have disproportionately large impacts on biodiversity, beyond what would be expected from area alone. The expansion and densification of built-up areas fragment riparian and coastal habitats, disrupt lateral connectivity between rivers and floodplains, and impair longitudinal and land-water exchange processes essential to many species' life cycles (He et al., 2024). Together, these changes hinder biodiversity recovery and erode habitat continuity and functional connectivity across some of Europe's most ecologically valuable landscapes (Eppink et al., 2004). At the same time, these land-use changes effectively "lock in" socio-economic exposure to current and future climate shocks, as trillions of euros in infrastructure and millions of residents are now permanently located in high-risk zones (Rentschler et al., 2023). Annual uninsured flood losses in the EU already reach an estimated 27 billion euros (Bellia et al., 2025), with projected regional GDP losses of up to 0.5% under future climate scenarios (Knittel et al., 2024). Ultimately, the conversion of cropland into urban land undermines both food security and natural buffering capacity against climate extremes, reducing Europe's climate resilience and flood-mitigation potential (EEA, 2024; Halecki & Młyński, 2025).

Our third main finding is that land-water interfaces are not uniform between regions inside and outside the EU+, and that their temporal dynamics also differ markedly between these two areas. Countries inside the EU+, on average, experienced more intensive urbanization within the land-water interface than neighboring non-EU+ countries. This can be partly explained by Western and Central European countries historically having higher population density, with major industrial activity and transportation infrastructure developed along major riverways (e.g., Rhine, Rhone, and their tributaries) and along coasts. Many regions in Eastern Europe lagged behind this development, historically, but also due to the diverging economic trajectories countries took in the West and in the former Eastern Bloc. After the breakdown of the Soviet Union, many Eastern European countries went through period of strong recession, rural outmigration, and agricultural abandonment (Prishchepov et al., 2012), explaining the later and more gradual land take inside land-water interfaces we find (Fig. 4). This was followed by a more rapid economic growth in the 2000s, coinciding with the opening of these economies to global markets and foreign investment (Hennig et al., 2015). This East-West contrast in the timing of land take in the land-water interface is clearly reflected in our results (Fig. 4D−E) and is well documented. For instance, after the end of socialism, a spike in construction along the Elbe and Danube corridors occurred in Germany, boosted by investments that did not reach other post-socialist regions until later (Kasanko et al., 2006).

Our work provides a first, workable definition of the land-water interface and how this can be translated into high-resolution maps that can serve as a baseline. This framework is far more than an academic exercise: it serves as a robust practical tool for tracking environmental change and identifying critical "pressure zones", such as urbanizing coastal deltas or rapidly developing lakeshores, that require policy attention and planning (Grabowski et al., 2022; Weissteiner et al., 2016). Considering that most major catchments in Europe span multiple countries and regions inside and outside the EU, our consistent continental baseline, our work can also help to move beyond fragmented national data and definitions to align management with the ambitious goals of the EU Biodiversity Strategy for 2030 and the Nature Restoration Law, which specifically calls for the reconnection of 25,000 km of free-flowing rivers (*EEC*, 2025; Stoffers et al., 2024). Conceptually, framing land-water interfaces as a cohesive analytical unit complements existing terrestrial and aquatic planning approaches by emphasizing their interdependence. Although floodplains, riverbanks, and coastal systems have long been subject to dedicated management, these efforts are frequently fragmented across sectors and governance scales. An explicit land-water interface perspective can therefore enhance coordination among urban planning, water management, and conservation, helping to safeguard zones that play a central role in climate resilience, nutrient regulation, and biodiversity movement (Grabowski et al., 2022).

While we used the best-available data and carried out extensive validation exercises and robustness checks, a few limitations of our work need to be mentioned. First, given the continental scale of our study, we utilized mainly global datasets, which involves a necessary trade-off between spatial coverage and spatial precision, specifically regarding spectrally complex environments like wetlands. Second, we delineated the land-water interface as a static baseline map, as most of our input datasets do not constitute time series. While our definition is generic, and most features such as geomorphology or lake shapes can be considered static over the time scale of decades, defining the land-water interface more dynamically would be beneficial, once the necessary data are available, to better account for changes such as sea-level rise or climate-driven water surface change (Pekel et al., 2016). Finally, while we quantify land transformation at the land-water interface, our analysis primarily focuses on cropland and built-up land. These two types of land best capture the dominant human activities of agriculture and urbanization, and they exhibit the greatest and most consistently detectable changes in our maps (Fig. S4). Other land-cover dynamics, such as cropland–grassland transitions, woody encroachment, and losses of semi-natural and natural habitats, are also likely important within the land-water interface. However, mapping these reliably would require substantial remote-sensing efforts beyond the scope of this study.

Land-water interfaces are of outstanding social-ecological importance, yet are often neglected in research and policy. We here provide a generic, robust, and operationalizable definition, along with a

transparent and reproducible workflow to map the land-water interface. This allowed us to uncover how an increasing land take in the land-water interface threatens to undermine food security and resilience against climate pressure, such as through flood risk. This also demonstrates that our concept and maps can provide a useful spatial architecture for a more dynamic, function-based monitoring system of these vulnerable transitional zones. Importantly, our methodology is highly scalable. By utilizing modular, open-access inputs, our workflow is easily transferable to other continents, including data-scarce regions, as well as to the global scale. This could help us better recognize land-water interfaces as ecologically indispensable and vulnerable ecotones that provide some of the planet's most vital green infrastructure.

Methods

Study area

Our study was the entire European continent, from the Atlantic to the Ural Mountains, encompassing all or portions of 57 countries and territories (Fig. S5). The area includes the entire European Union, the former Eastern Bloc (e.g., Ukraine, Belarus, and Georgia), as well as European Russia, all of Turkey, and the Caucasus Mountains. The region thus also covers broad bioclimatic gradients, from the Arctic tundra to the temperate Atlantic lowlands, the Mediterranean and subtropical forests at the Black Sea, and a variety of climates, from strongly oceanic to strongly continental.

The hydrographic network in this region traverses a wide range of climatic and topographic zones, and our region includes several major transboundary rivers and their catchments, including the Danube, Rhine, Elbe, Vistula, Dniester, and Po, which give rise to a highly varied pattern of flow regimes and watershed structures across the continent. The region is equally diverse in terms of socio-economic gradients, from densely settled regions to sparsely populated areas, and in terms of land use, with many regions characterized by intensive agriculture (e.g., Western European plains) while less intensive land use prevails in other areas (e.g., many regions of Eastern Europe and the former Soviet Union). This diversity makes the region an interesting testbed for mapping and analyzing the land-water interface.

Definition of land-water interface

We defined the land-water interface as the dynamic zone in which terrestrial and aquatic systems interact most closely (Fig. 5A). On the water side, the land-water interface covers the shallow edges close to the land area, including areas that are only seasonally exposed to water, such as shoreline marshes, reed beds, and mud and sandflats. On the land side, the land-water interface is the low-lying terrestrial area that stays connected to the adjacent river, lake, or ocean water body through spatial proximity and/or because floods, back-flow, or groundwater connect these areas (e.g., floodplains, deltas, and seasonally inundated

lowlands). Together, the water-side and land-side form a narrow belt, usually only 10s to 100s of meters wide, where ecological processes are linked. We applied this definition uniformly to rivers, lakes, and coastal areas.

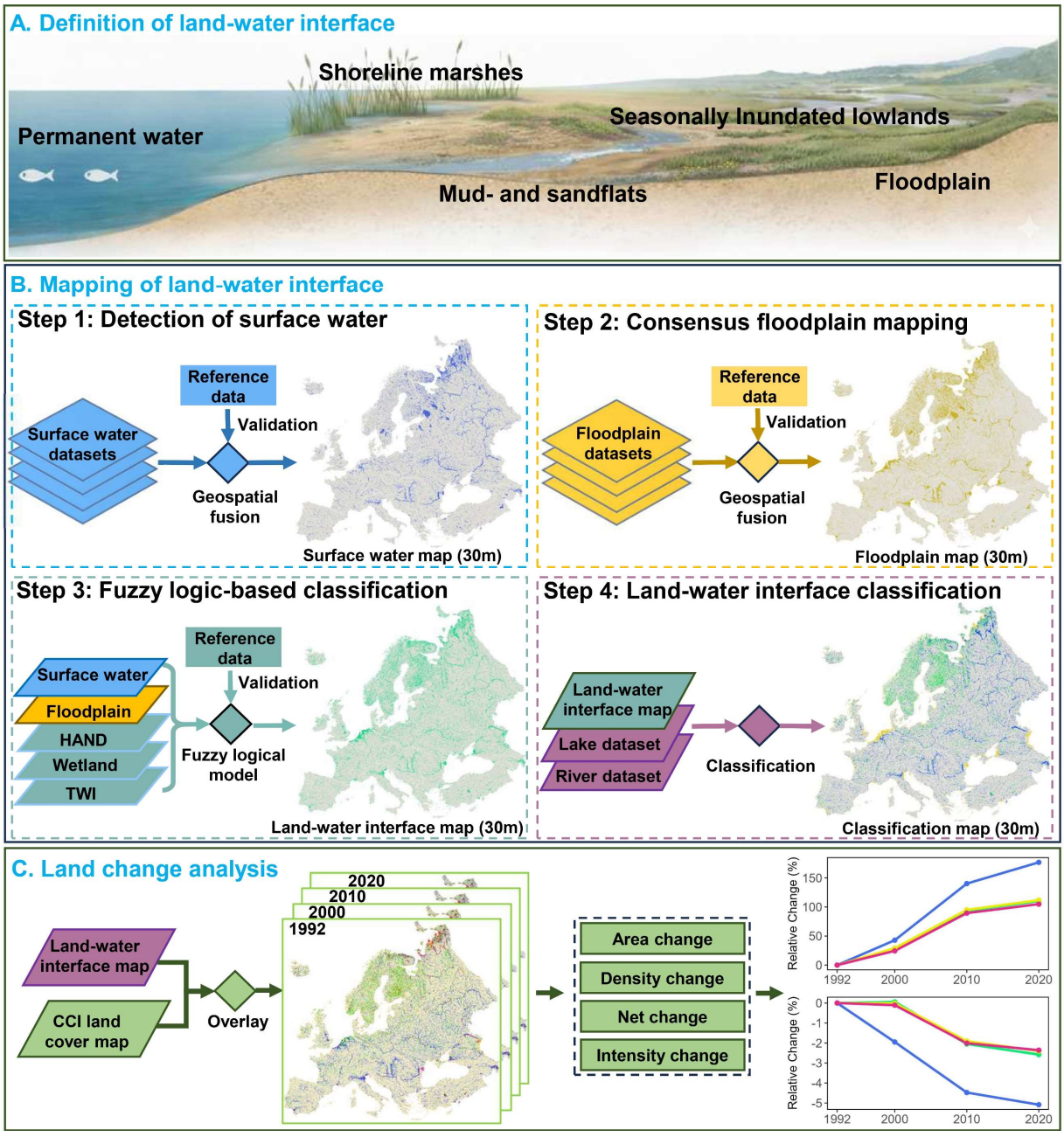

Figure 5. Conceptual framework and workflow for mapping the land-water interface and analyzing land changes within it. HAND: Height Above the Nearest Drainage; TWI: Topographic Wetness Index.

Mapping the land-water interface

To delineate the land-water interface, we integrated 20 geospatial datasets (see Table S1 for data sources and details on the datasets), capturing surface-water dynamics, inundation hazard, wetlands, shorelines, or terrain morphology. We prioritized products that are open-access and have high spatial resolution (<100 m), documented accuracy, and full continental coverage, thus keeping the workflow transparent, reproducible, and transferable. In the case of dynamic features, such as surface water and floodplains, no single map accurately captures these features. We thus adopted an anchor-plus-fusion strategy: (i) we selected the best-validated, highest-resolution map as an "anchor"; and then (ii) merged one or more complementary datasets with the anchor to minimize errors of omission and resolve misclassifications. All fusions were performed after reprojecting to a common 30-m grid. For other features, such as lakes, coastlines, and digital elevation models, we adopted the single most accurate and up-to-date dataset available, thereby limiting redundancy and compound uncertainty. Our overall approach to map the land-water interface and evaluate its accuracy and completeness consisted of four main steps (Fig. 5B).

First, we generated a homogenized map of surface water areas based on datasets capturing water bodies (Table S1). We embarked from the Global Surface Water Maximum Water Extent dataset (GSW-MWE; Pekel et al., 2016). To remove remaining artefacts and commission errors in this map, we created a consensus water mask from three broad-scale land-cover maps, namely, ESA World Cover 2020/2021 (WorldCover; Zanaga et al., 2021, 2022), Global Land-Cover Dynamics Monitoring Product (GLC-FCS30D; Zhang et al., 2024b), and Global annual wetland (GWL-FCS30D; Zhang et al., 2024a), retaining only GSW-MWE objects overlapping with the consensus water class from these maps. We then added water areas derived from the Sentinel-based World Cover and MERIT Hydro datasets (Yamazaki et al., 2019), improving the inclusion of narrow water bodies (e.g., rivers and streams). We validated this consensus map using an independent sample, following best-practice methodologies (Olofsson et al., 2014). The overall accuracy of our consensus water mask (F1 = 0.96) was substantially higher than that of the individual input datasets (see Supporting Information 1).

Our second step consisted of generating a consensus floodplain map, based on the fusion of five floodplain datasets. Our anchor for this analysis was the JRC River Flood Hazard Maps (RFHM; Baugh et al., 2024), representing a "1-in-100-year" inundation model, the most up-to-date validated hydraulic product for Europe (Dottori et al., 2022). We then used four additional datasets, the Potential Flood Prone Areas Extent (PFPAE; EEA 2020), GFPLAIN250m (GFPLAIN; Nardi et al., 2019), SHIFT Floodplain (SHIFT; Zheng et al., 2024), and Global Flood Database (GFD; Tellman et al., 2021), to address errors of commission in the anchor floodplain dataset. Specifically, a pixel was labelled as floodplain only if either the anchor and at least one auxiliary source agreed, or if all three auxiliary sources agreed on the categorization as floodplain. We finally merged this mask with the Global Coast Flood Map (GCF;

Vousdoukas 2023) dataset to ensure coverage of tidal floodplains. Again, we validated this consensus floodplain mask using 8,200 reference points sampled from local flood maps. This showed that our consensus map had high accuracy (F1= 0.74) and outperformed any individual input map (see Supporting Information 2).

Our third step involved a fuzzy logic-based geospatial model to map the land-water interface itself. Unlike binary classification schemes, fuzzy logic enables the continuous assessment of class membership, which is particularly advantageous for ecotones such as floodplains, riparian zones, and wetland margins, where boundaries are inherently diffuse (Weissteiner et al., 2016). We used five spatial variables: (1) Distance to surface water (D_{SW}), (2) Distance to flood-prone areas (D_{FP}), (3) Height Above the Nearest Drainage (HAND; Yamazaki et al. 2019), (4) Wetland probability (WP; Zhang et al. 2024a, Lehner et al. 2025), and (5) the Topographic Wetness Index (TWI; Amatulli et al. 2022). Each variable was transformed into a fuzzy membership value within the range [0,1], using monotonic linear scaling:

$$u_i(x) = \begin{cases} 1, & x \le a_i \\ \frac{b_i - x}{b_i - a_i}, & a_i < x < b_i \\ 0, & x \ge b_i \end{cases} \quad (1)$$

$$u_i(x) = \begin{cases} 0, & x \le a_i \\ \frac{x - a_i}{b_i - a_i}, & a_i < x < b_i \\ 0, & x \ge b_i \end{cases} \quad (2)$$

where $u_i(x)$ is the fuzzy membership score for variable i at a given value x. It ranges between 0 (no membership) and 1 (full membership). a_i is the lower threshold where full membership is assigned. b_i is the upper threshold where membership drops to zero. For variables that decrease the likelihood of being in the interface as the value grows (i.e., D_{SW}, D_{FP} and HAND) we use a descending linear ramp (1) and vice versa (2) for variables that increase the likelihood (i.e., WP and TWI). Then we applied a fuzzy-weighted mean (3):

$$S(x) = \sum_{i=1}^{5} w_i \cdot u_i(x) \quad (3)$$

where $S(x) \in [0,1]$ is the composite suitability score for belonging to the land-water interface, and w_i is the weight assigned to indicator i. Higher values of $S(x)$ indicate stronger overall evidence that pixel x belongs to the land-water interface. To delineate the land-water interface on the water side, we assigned full membership to all pixels representing seasonal water and additionally defined a nearshore water zone by applying an inward dilation of three pixels (≈90 m) from the shoreline into water bodies. This distance

was chosen to be consistent with the spatial resolution of the input data and to capture the immediate nearshore interface zone while minimizing inclusion of offshore or deep-water areas. Pixels within this buffered water strip were also assigned full membership. Because tidal flats are not consistently classified as water in seasonal water products due to tidal variability and surface conditions, we further used the 30-m wetlands classification map to identify and include any remaining coastal tidal-flat pixels not captured by the previous assignments. We applied a threshold of 0.6 to create the binary land-water interface map. This threshold was selected because it corresponds to pixels with consistently high membership across multiple indicators and provides an optimal balance between omission and commission errors.

Finally, we conducted a sample-based accuracy assessment using 2031 independent reference samples that were randomly selected across the full range of membership values. Each sample was visually interpreted using high-resolution Google Earth imagery and classified according to the presence of geomorphic or ecological features indicative of land-water interaction (e.g., shoreline wetlands, riparian corridors, floodplain features, or seasonal inundation signatures). Using these visually interpreted samples as reference labels, the threshold of 0.6 yielded the highest F1 score among tested thresholds, achieving an F1 score of 0.88, with a precision of 0.92 and a recall of 0.85 (see Supporting Information 3).

Our final step consisted of subdividing the generic land-water interface map into coastal, river, and lake interface classes. Coastal interfaces were defined using a two-tier coastal zone: (i) a 2-km inland buffer from the EEA coastline (EEA, 2017) without an elevation constraint and (ii) an additional zone within 10-km of the coastline limited to elevations <10-m based on DEM data (Hawker et al., 2022; Pronk et al., 2024). All land-water interface pixels within this zone were assigned to the coastal class, with targeted manual extensions upstream in major estuaries where clear tidal/estuarine morphology (e.g., funnel-shaped channels, tidal flats, salt marshes) indicated tidal influence beyond 10-km. The remaining inland land-water interface was split into riverine and lacustrine classes using a connectivity- and patch-based workflow: we dilated the inland land-water interface (without removing permanent water) by three pixels (~90-m) to create a connected river-candidate mask, polygonised it, removed patches < 2-km², and applied adaptive area–shape thresholds to exclude lake-like patches, supported by consistent visual checks in high-resolution Google Earth imagery. To refine lake/reservoir separation where lakes were connected to rivers, we used GLRSED (Bai et al., 2025) and HydroLAKES (Messager et al., 2016) to delineate lake/reservoir water bodies, split reservoirs at dam crests to retain only upstream lacustrine portions, buffered these polygons, and masked them out from the river-candidate mask. We finalized the riverine interface mask through a final visual inspection and minor manual edits. All non-coastal inland land-water interface pixels not included in this finalized riverine mask were then classified as lacustrine interface. Further details are provided in Supporting Information 4.

Land transformations in the land-water interface

To analyze changes in cropland and built-up areas in the land-water interface, we used the ESA Climate Change Initiative (CCI) Land-Cover series (1992−2020), which offers seamless global annual coverage at 300-m resolution, has undergone extensive peer-reviewed validation, and is widely used in land-cover-change analyses (Rajib et al., 2023). We collapsed all CCI classes into the six land categories: Cropland, Forest, Grassland, Wetland, Built-up, and Others. We then quantified land-cover changes for four reference years (1992, 2000, 2010, and 2020) for the land-water interface. We derived (i) total area (km^2), (ii) density of built-up or cropland (expressed as the fraction of cell area, ‰), (iii) absolute change (Δ area, km^2) between successive time steps, and (iv) cumulative percentage change relative to the 1992 baseline. We computed these metrics for each land-water interface subtype (river, lake, and coast), and for the EU+ vs. non-EU+ regions (see Supplementary Information 5 for details).

We further implemented the Intensity Analysis framework (Aldwaik & Pontius, 2012) to evaluate land-cover changes at the category and transition levels. At the category level, we quantified gross gains and losses for each land-cover class. We then applied the transition level to identify the specific sources of these gains, for example, by determining which land-cover types were preferentially converted to built-up areas. This analysis compares the observed intensity, defined as the annual rate of a specific land-cover transition, with the uniform intensity, which represents the expected rate of gain for a given category if its expansion were proportional to the availability of all non-gaining land-cover classes. Effectively acting as an area-weighted baseline, the uniform intensity describes a hypothetical scenario in which the gaining category expands indiscriminately across the landscape. When the observed intensity of a transition (e.g., cropland → built-up) exceeds the uniform intensity of the gaining category, the transition can be interpreted as systematic targeting rather than proportional expansion. The Intensity Analysis framework were performed in R using the *OpenLand* package (Exavier & Zeilhofer, 2020).

Acknowledgements

We thank Dr. Mirela G. Tulbure and Dr. Sami Domisch for their insights on mapping and validating the land-water interface. This study was funded by the Horizon Europe research and innovation programmes (wildE, grant number 101081251 and DANUBE4all project, grant number 101093985), as well as the Leibniz Competition project “Freshwater Megafauna Futures”. SCJ considers it a contribution to the Collaborative Research Centre 1439 RESIST funded by the Deutsche Forschungsgemeinschaft (DFG, German Research Foundation, CRC 1439/2, project number: 426547801).

Data availability

The source code for processing input data and mapping the land-water interface is available at: https://github.com/XiangLIUll/Land-water-interface. The land-water interface maps can be explored at http://hu.berlin/LWI

References

Acreman, M., & Holden, J. (2013). How Wetlands Affect Floods. *Wetlands*, *33*(5), 773–786. https://doi.org/10.1007/s13157-013-0473-2

Aldwaik, S. Z., & Pontius, R. G. (2012). Intensity analysis to unify measurements of size and stationarity of land changes by interval, category, and transition. *Landscape and Urban Planning*, *106*(1), 103–114. https://doi.org/10.1016/j.landurbplan.2012.02.010

Altanov, V. Y., Jähnig, S. C., & He, F. (2025). A systematic map of hydropower impacts on megafauna at the land-water interface. *Biological Conservation*, *305*, 111092. https://doi.org/10.1016/j.biocon.2025.111092

Amatulli, G., Garcia Marquez, J., Sethi, T., Kiesel, J., Grigoropoulou, A., Üblacker, M. M., Shen, L. Q., & Domisch, S. (2022). Hydrography90m: A new high-resolution global hydrographic dataset. *Earth System Science Data*, *14*(10), 4525–4550. https://doi.org/10.5194/essd-14-4525-2022

Andreadis, K. M., Wing, O. E. J., Colven, E., Gleason, C. J., Bates, P. D., & Brown, C. M. (2022). Urbanizing the floodplain: Global changes of imperviousness in flood-prone areas. *Environmental Research Letters*, *17*(10), 104024. https://doi.org/10.1088/1748-9326/ac9197

Bai, B., Mu, L., & Tan, Y. (2025). A Global Lakes/Reservoirs Surface Extent Dataset (GLRSED): An Integration of Multi-Source Data. *Geoscience Data Journal*, *12*(1), e285. https://doi.org/10.1002/gdj3.285

Bastino, V., Boughaba, J., & van de Bund, W. (2021). Biodiversity strategy 2030 barrier removal for river restoration. *European Commission. Luxembourg*.

Baugh, C., Colonese, J., D'Angelo, C., Dottori, F., Neal, J., Prudhomme, C., & Salamon, P. (2024). *Global river flood hazard maps*. http://data.europa.eu/89h/jrc-floods-floodmapgl_rp50y-tif

Bellia, M., Di Girolamo, E. F., Pagano, A., & Giudici, M. P. (2025). The flood protection gap: Evidence for public finances and insurance premiums. *Risk Management and Insurance Review*, *28*(1), 34–66. https://doi.org/10.1111/rmir.70001

Brandolini, F., & Cremaschi, M. (2018). The Impact of Late Holocene Flood Management on the Central Po Plain (Northern Italy). *Sustainability*, *10*(11). https://doi.org/10.3390/su10113968

Bren d'Amour, C., Reitsma, F., Baiocchi, G., Barthel, S., Güneralp, B., Erb, K.-H., Haberl, H., Creutzig, F., & Seto, K. C. (2017). Future urban land expansion and implications for global croplands. *Proceedings of the National Academy of Sciences*, *114*(34), 8939–8944. https://doi.org/10.1073/pnas.1606036114

Bruisch, K. (2020). Nature Mistaken: Resource-Making, Emotions and the Transformation of Peatlands in the Russian Empire and the Soviet Union. *Environment and History*, *26*(3), 359–382. https://www.jstor.org/stable/27078135

Campbell, A. D., Fatoyinbo, L., Goldberg, L., & Lagomasino, D. (2022). Global hotspots of salt marsh change and carbon emissions. *Nature*, *612*(7941), 701–706. https://doi.org/10.1038/s41586-022-05355-z

Capon, S. J., Chambers, L. E., Mac Nally, R., Naiman, R. J., Davies, P., Marshall, N., Pittock, J., Reid, M., Capon, T., Douglas, M., Catford, J., Baldwin, D. S., Stewardson, M., Roberts, J., Parsons, M., & Williams, S. E. (2013). Riparian Ecosystems in the 21st Century: Hotspots for Climate Change Adaptation? *Ecosystems*, *16*(3), 359–381. https://doi.org/10.1007/s10021-013-9656-1

Chipps, S. R., Hubbard, D. E., Werlin, K. B., Haugerud, N. J., Powell, K. A., Thompson, J., & Johnson, T. (2006). Association between wetland disturbance and biological attributes in floodplain wetlands. *Wetlands*, *26*(2), 497–508. https://doi.org/10.1672/0277-5212(2006)26%255B497:ABWDAB%255D2.0.CO;2

Christiansen, T., Azlak, M., & Ivits-Wasser, E. (2019). *Floodplains: A natural system to preserve and restore.*

Copernicus Land Monitoring Service. (n.d.). *Coastal Zones*. Retrieved February 25, 2026, from https://land.copernicus.eu/en/products/coastal-zones

Dottori, F., Alfieri, L., Bianchi, A., Skoien, J., & Salamon, P. (2022). A new dataset of river flood hazard maps for Europe and the Mediterranean Basin. *Earth System Science Data*, *14*(4), 1549–1569. https://doi.org/10.5194/essd-14-1549-2022

Downing, J. P., Meybeck, M., Orr, J. C., Twilley, R. R., & Scharpenseel, H. W. (1993). Land and water interface zones. *Water, Air, and Soil Pollution*, *70*(1), 123–137. https://doi.org/10.1007/BF01104992

EEA. (2017). *EEA coastline for analysis*. https://www.eea.europa.eu/en/datahub/datahubitem-view/af40333f-9e94-4926-a4f0-0a787f1d2b8f?activeAccordion=945677

EEA. (2020a). *EEA potential flood-prone area extent*. https://www.eea.europa.eu/en/datahub/datahubitem-view/254a8583-e34f-4324-bbdf-1fbda7a3d222?activeAccordion=

EEA. (2020b). *Floodplains: A natural system to preserve and restore*. https://www.eea.europa.eu/en/analysis/publications/floodplains-a-natural-system-to-preserve-and-restore

EEA. (2024). *Europe's state of water 2024: The need for improved water resilience*. https://www.eea.europa.eu/en/analysis/publications/europes-state-of-water-2024

EEC. (2025, October 23). https://environment.ec.europa.eu/strategy/biodiversity-strategy-2030_en

Eppink, F. V., van den Bergh, J. C. J. M., & Rietveld, P. (2004). Modelling biodiversity and land use: Urban growth, agriculture and nature in a wetland area. *Ecological Economics*, *51*(3), 201–216. https://doi.org/10.1016/j.ecolecon.2004.04.011

Ervin, G. N., & Wetzel, R. G. (2003). An ecological perspective of allelochemical interference in land–water interface communities. *Plant and Soil*, *256*(1), 13–28. https://doi.org/10.1023/A:1026253128812

Estel, S., Kuemmerle, T., Alcántara, C., Levers, C., Prishchepov, A., & Hostert, P. (2015). Mapping farmland abandonment and recultivation across Europe using MODIS NDVI time series. *Remote Sensing of Environment*, *163*, 312–325. https://doi.org/10.1016/j.rse.2015.03.028

European Environment Agency. (2021). *Riparian Zones Land Cover/Land Use 2018 (vector), Europe, 6-yearly, Dec. 2021* (Version 01.00) [SHP]. European Environment Agency. https://doi.org/10.2909/2AFCA4EC-76E2-4155-B4E6-7460F9F6AE01

Exavier, R., & Zeilhofer, P. (2020). *OpenLand: Software for quantitative analysis and visualization of land use and cover change*.

Fernandes, M. R., Aguiar ,Francisca Constança, Ferreira ,Maria Teresa, & and Pereira, J. M. C. (2013). Spectral separability of riparian forests from small and medium-sized rivers across a latitudinal gradient using multispectral imagery. *International Journal of Remote Sensing*, *34*(7), 2375–2401. https://doi.org/10.1080/01431161.2012.744491

574 Fernandes, M. R., Segurado, P., Jauch, E., & Ferreira, M. T. (2016). Riparian responses to extreme climate and
575 land-use change scenarios. *Science of The Total Environment*, *569–570*, 145–158.
576 https://doi.org/10.1016/j.scitotenv.2016.06.099
577 Firth, A., Firth, E., Rothero, E., & Gowing, D. (2026). Historic Floodplain Meadows in the Landscape:
578 Investigating Anthropogenic Habitats Important for Nature Conservation, Carbon Sequestration and Flood
579 Attenuation. *Environmental Management*, *76*(3), 106. https://doi.org/10.1007/s00267-026-02396-2
580 Fischer, R. A., & Fischenich, J. C. (2000). *Design Recommendations for Riparian Corridors and Vegetated*
581 *Buffer Strips*.
582 Fluet-Chouinard, E., Stocker, B. D., Zhang, Z., Malhotra, A., Melton, J. R., Poulter, B., Kaplan, J. O., Goldewijk,
583 K. K., Siebert, S., Minayeva, T., Hugelius, G., Joosten, H., Barthelmes, A., Prigent, C., Aires, F., Hoyt, A.
584 M., Davidson, N., Finlayson, C. M., Lehner, B., … McIntyre, P. B. (2023). Extensive global wetland loss
585 over the past three centuries. *Nature*, *614*(7947), 281–286. https://doi.org/10.1038/s41586-022-05572-6
586 Furgała-Selezniow, G., Jankun-Woźnicka, M., & Mika, M. (2020). Lake regions under human pressure in the
587 context of socio-economic transition in Central-Eastern Europe: The case study of Olsztyn Lakeland,
588 Poland. *Land Use Policy*, *90*, 104350. https://doi.org/10.1016/j.landusepol.2019.104350
589 Furgała-Selezniow, G., Jankun-Woźnicka, M., Woźnicki, P., Cai, X., Erdei, T., & Boromisza, Z. (2022). Trends
590 in Lakeshore Zone Development: A Comparison of Polish and Hungarian Lakes over 30-Year Period.
591 *International Journal of Environmental Research and Public Health*, *19*(4), 2141.
592 https://doi.org/10.3390/ijerph19042141
593 Gardi, C., Panagos, P., Van Liedekerke, M., Bosco, C., & De Brogniez, D. (2015). Land take and food security:
594 Assessment of land take on the agricultural production in Europe. *Journal of Environmental Planning and*
595 *Management*, *58*(5), 898–912. https://doi.org/10.1080/09640568.2014.899490
596 Gatejel, L. (2025). Turning wetlands into "Productive" spaces: Modernization and sustainable rural development
597 in Romania, 1900–1945. *Water History*. https://doi.org/10.1007/s12685-025-00371-y
598 Giri, S., & Qiu, Z. (2016). Understanding the relationship of land uses and water quality in Twenty First Century:
599 A review. *Journal of Environmental Management*, *173*, 41–48.
600 https://doi.org/10.1016/j.jenvman.2016.02.029
601 González del Tánago, M., Martínez-Fernández, V., Aguiar, F. C., Bertoldi, W., Dufour, S., García de Jalón, D.,
602 Garófano-Gómez, V., Mandzukovski, D., & Rodríguez-González, P. M. (2021). Improving river
603 hydromorphological assessment through better integration of riparian vegetation: Scientific evidence and
604 guidelines. *Journal of Environmental Management*, *292*, 112730.
605 https://doi.org/10.1016/j.jenvman.2021.112730
606 Gosnell, H., & Abrams, J. (2011). Amenity migration: Diverse conceptualizations of drivers, socioeconomic
607 dimensions, and emerging challenges. *GeoJournal*, *76*(4), 303–322. https://doi.org/10.1007/s10708-009-
608 9295-4
609 Grabowski, R. C., Vercruysse, K., Holman, I., Azhoni, A., Bala, B., Shankar, V., Beale, J., Mukate, S., Poddar,
610 A., Peng, J., & Meersmans, J. (2022). The land–river interface: A conceptual framework of environmental
611 process interactions to support sustainable development. *Sustainability Science*, *17*(4), 1677–1693.
612 https://doi.org/10.1007/s11625-022-01150-x
613 Halecki, W., & Młyński, D. (2025). Urban flood dilemmas: How European cities growth shapes flood risk and
614 resilience strategies? *Journal of Environmental Management*, *374*, 124161.
615 https://doi.org/10.1016/j.jenvman.2025.124161

Hall, C. M. (2001). Trends in ocean and coastal tourism: The end of the last frontier? *Ocean & Coastal Management, Trends in Ocean Industries*, *44*(9), 601–618. https://doi.org/10.1016/S0964-5691(01)00071-0

Hawker, L., Uhe, P., Paulo, L., Sosa, J., Savage, J., Sampson, C., & Neal, J. (2022). A 30 m global map of elevation with forests and buildings removed. *Environmental Research Letters*, *17*(2), 024016. https://doi.org/10.1088/1748-9326/ac4d4f

He, F., Svenning, J.-C., Chen, X., Tockner, K., Kuemmerle, T., le Roux, E., Moleón, M., Gessner, J., & Jähnig, S. C. (2024). Freshwater megafauna shape ecosystems and facilitate restoration. *Biological Reviews*, *99*(4), 1141–1163. https://doi.org/10.1111/brv.13062

Hennig, E. I., Schwick, C., Soukup, T., Orlitová, E., Kienast, F., & Jaeger, J. A. G. (2015). Multi-scale analysis of urban sprawl in Europe: Towards a European de-sprawling strategy. *Land Use Policy*, *49*, 483–498. https://doi.org/10.1016/j.landusepol.2015.08.001

Hoffmann, R. C. (2005). A brief history of aquatic resource use in medieval Europe. *Helgoland Marine Research*, *59*(1), 22–30. https://doi.org/10.1007/s10152-004-0203-5

Johansen, K., Phinn, S., & Witte, C. (2010). Mapping of riparian zone attributes using discrete return LiDAR, QuickBird and SPOT-5 imagery: Assessing accuracy and costs. *Remote Sensing of Environment*, *114*(11), 2679–2691. https://doi.org/10.1016/j.rse.2010.06.004

Jongman, B., Hochrainer-Stigler, S., Feyen, L., Aerts, J. C. J. H., Mechler, R., Botzen, W. J. W., Bouwer, L. M., Pflug, G., Rojas, R., & Ward, P. J. (2014). Increasing stress on disaster-risk finance due to large floods. *Nature Climate Change*, *4*(4), 264–268. https://doi.org/10.1038/nclimate2124

Karr, J. R., & Schlosser, I. J. (1978). Water Resources and the Land-Water Interface. *Science*, *201*(4352), 229–234. https://doi.org/10.1126/science.201.4352.229

Kasanko, M., Lavalle, C., Barredo, C., Sagris, V., Petrov, L., Uhel, R., Ludlow, D., Fons, J., Gomez, O., & Blanes, N. (2006). *Urban sprawl in Europe-The ignored challenge*.

Kastner, T., Matej, S., Forrest, M., Gingrich, S., Haberl, H., Hickler, T., Krausmann, F., Lasslop, G., Niedertscheider, M., Plutzar, C., Schwarzmüller, F., Steinkamp, J., & Erb, K.-H. (2022). Land use intensification increasingly drives the spatiotemporal patterns of the global human appropriation of net primary production in the last century. *Global Change Biology*, *28*(1), 307–322. https://doi.org/10.1111/gcb.15932

Knittel, N., Tesselaar, M., Wouter Botzen, W. J., Bachner, G., & Tiggeloven, T. (2024). Who bears the indirect costs of flood risk? An economy-wide assessment of different insurance systems in Europe under climate change. *Economic Systems Research*, *36*(1), 131–160. https://doi.org/10.1080/09535314.2023.2272211

Kuemmerle, T., Levers, C., Erb, K., Estel, S., Jepsen, M. R., Müller, D., Plutzar, C., Stürck, J., Verkerk, P. J., Verburg, P. H., & Reenberg, A. (2016). Hotspots of land use change in Europe. *Environmental Research Letters*, *11*(6), 064020. https://doi.org/10.1088/1748-9326/11/6/064020

Kuemmerle, T., Olofsson, P., Chaskovskyy, O., Baumann, M., Ostapowicz, K., Woodcock, C. E., Houghton, R. A., Hostert, P., Keeton, W. S., & Radeloff, V. C. (2011). Post-Soviet farmland abandonment, forest recovery, and carbon sequestration in western Ukraine. *Global Change Biology*, *17*(3), 1335–1349. https://doi.org/10.1111/j.1365-2486.2010.02333.x

Lehner, B., Anand, M., Fluet-Chouinard, E., Tan, F., Aires, F., Allen, G. H., Bousquet, P., Canadell, J. G., Davidson, N., Ding, M., Finlayson, C. M., Gumbricht, T., Hilarides, L., Hugelius, G., Jackson, R. B., Korver, M. C., Liu, L., McIntyre, P. B., Nagy, S., … Thieme, M. (2025). Mapping the world's inland

surface waters: An upgrade to the Global Lakes and Wetlands Database (GLWD v2). *Earth System Science Data*, *17*(6), 2277–2329. https://doi.org/10.5194/essd-17-2277-2025

Levers, C., Müller, D., Erb, K., Haberl, H., Jepsen, M. R., Metzger, M. J., Meyfroidt, P., Plieninger, T., Plutzar, C., Stürck, J., Verburg, P. H., Verkerk, P. J., & Kuemmerle, T. (2018). Archetypical patterns and trajectories of land systems in Europe. *Regional Environmental Change*, *18*(3), 715–732. https://doi.org/10.1007/s10113-015-0907-x

MacManus, K., Balk, D., Engin, H., McGranahan, G., & Inman, R. (2021). Estimating population and urban areas at risk of coastal hazards, 1990–2015: How data choices matter. *Earth System Science Data*, *13*(12), 5747–5801. https://doi.org/10.5194/essd-13-5747-2021

McGranahan, G., Balk, D., & Anderson, B. (2007). The rising tide: Assessing the risks of climate change and human settlements in low elevation coastal zones. *Environment & Urbanization*, *19*(1), 17–37. https://doi.org/10.1177/0956247807076960

Messager, M. L., Lehner, B., Grill, G., Nedeva, I., & Schmitt, O. (2016). Estimating the volume and age of water stored in global lakes using a geo-statistical approach. *Nature Communications*, *7*(1), 13603. https://doi.org/10.1038/ncomms13603

Naiman, R. J., Decamps, H., & McClain, M. E. (2010). *Riparia: Ecology, Conservation, and Management of Streamside Communities*. Elsevier.

Nardi, F., Annis, A., Di Baldassarre, G., Vivoni, E. R., & Grimaldi, S. (2019). GFPLAIN250m, a global high-resolution dataset of Earth's floodplains. *Scientific Data*, *6*(1), 180309. https://doi.org/10.1038/sdata.2018.309

Neumann, B., Vafeidis, A. T., Zimmermann, J., & Nicholls, R. J. (2015). Future Coastal Population Growth and Exposure to Sea-Level Rise and Coastal Flooding—A Global Assessment. *PLOS ONE*, *10*(3), e0118571. https://doi.org/10.1371/journal.pone.0118571

Nordio, G., Frederiks, R., Hingst, M., Carr, J., Kirwan, M., Gedan, K., Michael, H., & Fagherazzi, S. (2023). Frequent Storm Surges Affect the Groundwater of Coastal Ecosystems. *Geophysical Research Letters*, *50*(1), e2022GL100191. https://doi.org/10.1029/2022GL100191

Olofsson, P., Foody, G. M., Herold, M., Stehman, S. V., Woodcock, C. E., & Wulder, M. A. (2014). Good practices for estimating area and assessing accuracy of land change. *Remote Sensing of Environment*, *148*, 42–57. https://doi.org/10.1016/j.rse.2014.02.015

Pace, G., Gutiérrez-Cánovas, C., Henriques, R., Carvalho-Santos, C., Cássio, F., & Pascoal, C. (2022). Remote sensing indicators to assess riparian vegetation and river ecosystem health. *Ecological Indicators*, *144*, 109519. https://doi.org/10.1016/j.ecolind.2022.109519

Pekel, J.-F., Cottam, A., Gorelick, N., & Belward, A. S. (2016). High-resolution mapping of global surface water and its long-term changes. *Nature*, *540*(7633), 418–422. https://doi.org/10.1038/nature20584

Petrovszki, J., Szilassi, P., & Erős, T. (2024). Mass tourism generated urban land expansion in the catchment of Lake Balaton, Hungary – analysis of long-term changes in characteristic socio-political periods. *Land Use Policy*, *142*, 107185. https://doi.org/10.1016/j.landusepol.2024.107185

Prishchepov, A. V., Radeloff, V. C., Baumann, M., Kuemmerle, T., & Müller, D. (2012). Effects of institutional changes on land use: Agricultural land abandonment during the transition from state-command to market-driven economies in post-Soviet Eastern Europe. *Environmental Research Letters*, *7*(2), 024021. https://doi.org/10.1088/1748-9326/7/2/024021

699 Pronk, M., Hooijer, A., Eilander, D., Haag, A., de Jong, T., Vousdoukas, M., Vernimmen, R., Ledoux, H., &
700 Eleveld, M. (2024). DeltaDTM: A global coastal digital terrain model. *Scientific Data*, *11*(1), 273.
701 https://doi.org/10.1038/s41597-024-03091-9
702 Quast, J. (2005). Reasons for historical hydraulic engineering measures for the draining of the Oderbruch and
703 their valuation in today's view. *German Water History Association, Integrated Land and Water Resources*
704 *Management in History, Schriften Der DWhG, Sonderband*, *2*, 115–122.
705 Rajib, A., Zheng, Q., Lane, C. R., Golden, H. E., Christensen, J. R., Isibor, I. I., & Johnson, K. (2023). Human
706 alterations of the global floodplains 1992–2019. *Scientific Data*, *10*(1), 499.
707 https://doi.org/10.1038/s41597-023-02382-x
708 Rentschler, J., Avner, P., Marconcini, M., Su, R., Strano, E., Vousdoukas, M., & Hallegatte, S. (2023). Global
709 evidence of rapid urban growth in flood zones since 1985. *Nature*, *622*(7981), 87–92.
710 https://doi.org/10.1038/s41586-023-06468-9
711 Rosati, R. M. (2025). Urban Sprawl and Routing: A Comparative Study on 156 European Cities. *Landscape and*
712 *Urban Planning*, *253*, 105205. https://doi.org/10.1016/j.landurbplan.2024.105205
713 Rutledge, D., Briggs, C., & Price, R. (2007). *Condition and Trend of Terrestrial Coastal Environments*.
714 Schierhorn, F., Müller, D., Beringer, T., Prishchepov, A. V., Kuemmerle, T., & Balmann, A. (2013). Post-Soviet
715 cropland abandonment and carbon sequestration in European Russia, Ukraine, and Belarus. *Global*
716 *Biogeochemical Cycles*, *27*(4), 1175–1185. https://doi.org/10.1002/2013GB004654
717 Schweizer, V., Colloff, M. J., & Pittock, J. (2022). The Dammed and the Saved: A Conservation Triage
718 Framework for Wetlands under Climate Change in the Murray–Darling Basin, Australia. *Environmental*
719 *Management*, *70*(4), 549–564. https://doi.org/10.1007/s00267-022-01692-x
720 Sonderegger, R., & Bätzing, W. (2013). Second homes in the Alpine Region: On the interplay between leisure,
721 tourism, outmigration and second homes in the Alps. *Revue de Géographie Alpine*, (Hors-Série).
722 https://doi.org/10.4000/rga.2511
723 Stanimirova, R., Tarrio, K., Turlej, K., McAvoy, K., Stonebrook, S., Hu, K.-T., Arévalo, P., Bullock, E. L.,
724 Zhang, Y., Woodcock, C. E., Olofsson, P., Zhu, Z., Barber, C. P., Souza, C. M., Chen, S., Wang, J. A.,
725 Mensah, F., Calderón-Loor, M., Hadjikakou, M., … Friedl, M. A. (2023). A global land cover training
726 dataset from 1984 to 2020. *Scientific Data*, *10*(1), 879. https://doi.org/10.1038/s41597-023-02798-5
727 Stoffers, T., Altermatt, F., Baldan, D., Bilous, O., Borgwardt, F., Buijse, A. D., Bondar-Kunze, E., Cid, N., Erős,
728 T., Ferreira, M. T., Funk, A., Haidvogl, G., Hohensinner, S., Kowal, J., Nagelkerke, L. A. J., Neuburg, J.,
729 Peller, T., Schmutz, S., Singer, G. A., … Hein, T. (2024). Reviving Europe's rivers: Seven challenges in
730 the implementation of the Nature Restoration Law to restore free-flowing rivers. *WIREs Water*, *11*(3),
731 e1717. https://doi.org/10.1002/wat2.1717
732 Tellman, B., Sullivan, J. A., Kuhn, C., Kettner, A. J., Doyle, C. S., Brakenridge, G. R., Erickson, T. A., &
733 Slayback, D. A. (2021). Satellite imaging reveals increased proportion of population exposed to floods.
734 *Nature*, *596*(7870), 80–86. https://doi.org/10.1038/s41586-021-03695-w
735 Tesselaar, M., Botzen, W. J. W., Tiggeloven, T., & Aerts, J. C. J. H. (2023). Flood insurance is a driver of
736 population growth in European floodplains. *Nature Communications*, *14*(1), 7483.
737 https://doi.org/10.1038/s41467-023-43229-8
738 Tockner, K., & Stanford, J. A. (2002). Riverine flood plains: Present state and future trends. *Environmental*
739 *Conservation*, *29*(3), 308–330.
740 Valenzuela-Martin, P., Miguel, S. M. de, Villar-Navascués, R., Gálvez-Pérez, D., Abad, B. G., & Bañón, L.
741 (2025). Explanatory factors for the distribution of short-term rentals in coastal destinations: The impact of

second homes in Alicante. *Journal of Policy Research in Tourism, Leisure and Events*, *17*(4), 1056–1074. https://doi.org/10.1080/19407963.2025.2466192

van Vliet, J., Eitelberg, D. A., & Verburg, P. H. (2017). A global analysis of land take in cropland areas and production displacement from urbanization. *Global Environmental Change*, *43*, 107–115. https://doi.org/10.1016/j.gloenvcha.2017.02.001

Verhoeven, J. T. A. (2014). Wetlands in Europe: Perspectives for restoration of a lost paradise. *Ecological Engineering, Wetland Restoration– Challenges and Opportunities*, *66*, 6–9. https://doi.org/10.1016/j.ecoleng.2013.03.006

Verhoeven, J. T. A., Arheimer, B., Yin, C., & Hefting, M. M. (2006). Regional and global concerns over wetlands and water quality. *Trends in Ecology & Evolution*, *21*(2), 96–103. https://doi.org/10.1016/j.tree.2005.11.015

Vousdoukas, M. (2023). *Global coastal flood maps* [Dataset]. Zenodo. https://zenodo.org/records/8057902

Ward, J. V., Tockner, K., Arscott, D. B., & Claret, C. (2002). Riverine landscape diversity. *Freshwater Biology*, *47*(4), 517–539. https://doi.org/10.1046/j.1365-2427.2002.00893.x

Weissteiner, C. J., Ickerott, M., Ott, H., Probeck, M., Ramminger, G., Clerici, N., Dufourmont, H., & De Sousa, A. M. R. (2016). Europe's Green Arteries—A Continental Dataset of Riparian Zones. *Remote Sensing*, *8*(11), Article 11. https://doi.org/10.3390/rs8110925

Wetlands International Europe. (2025, May 15). *Peatlands Passport—A Tour of Peatland Types*. Wetlands International Europe. https://europe.wetlands.org/peatlands-passport-a-tour-of-peatland-types/

Wolf, S., Esser, V., Schüttrumpf, H., & Lehmkuhl, F. (2021). Influence of 200 years of water resource management on a typical central European river. Does industrialization straighten a river? *Environmental Sciences Europe*, *33*(1), 15. https://doi.org/10.1186/s12302-021-00460-8

Yamazaki, D., Ikeshima, D., Sosa, J., Bates, P. D., Allen, G. H., & Pavelsky, T. M. (2019). MERIT Hydro: A High-Resolution Global Hydrography Map Based on Latest Topography Dataset. *Water Resources Research*, *55*(6), 5053–5073. https://doi.org/10.1029/2019WR024873

Yang, H., Niu, L., & van Vliet, J. (2026). Diverging trajectories of built-up land dynamics for country groups by income until 2100. *Habitat International*, *168*, 103677. https://doi.org/10.1016/j.habitatint.2025.103677

Zanaga, D., Van De Kerchove, R., Daems, D., De Keersmaecker, W., Brockmann, C., Kirches, G., Wevers, J., Cartus, O., Santoro, M., & Fritz, S. (2022). *ESA WorldCover 10 m 2021 v200*.

Zhang, X., Liu, L., Zhao, T., Wang, J., Liu, W., & Chen, X. (2024). Global annual wetland dataset at 30 m with a fine classification system from 2000 to 2022. *Scientific Data*, *11*(1), 310. https://doi.org/10.1038/s41597-024-03143-0

Zhang, X., Zhao, T., Xu, H., Liu, W., Wang, J., Chen, X., & Liu, L. (2024). GLC_FCS30D: The first global 30 m land-cover dynamics monitoring product with a fine classification system for the period from 1985 to 2022 generated using dense-time-series Landsat imagery and the continuous change-detection method. *Earth System Science Data*, *16*(3), 1353–1381. https://doi.org/10.5194/essd-16-1353-2024

Zheng, K., Lin, P., & Yin, Z. (2024). SHIFT: A spatial-heterogeneity improvement in DEM-based mapping of global geomorphic floodplains. *Earth System Science Data*, *16*(8), 3873–3891. https://doi.org/10.5194/essd-16-3873-2024